Ab initio–driven trajectory-based nuclear quantum dynamics in phase space

Ivano Tavernelli*

Laboratory of Computational Chemistry and Biochemistry, Ecole Polytechnique Fédérale de Lausanne, CH-1015 Lausanne, Switzerland

(Received 18 June 2012; revised manuscript received 28 January 2013; published 2 April 2013)

We derive a Bohmian trajectory-based quantum dynamics approach for the calculation of adiabatic and nonadiabatic quantum effects in *ab initio* on-the-fly molecular dynamics simulations. The method is designed for calculations in the full, unconstrained, phase space of molecular systems described within density functional theory and time-dependent density functional theory. The problem of solving quantum hydrodynamic equations using trajectories in high dimensions is addressed using an expansion of the nuclear amplitude in atom centered Gaussians that are propagated along the quantum trajectories. In this work, we investigate the adiabatic limit of this theory, even though the full nonadiabatic case is derived. The method is first tested on the H_2 molecule and then applied to the study of the proton transfer dynamics in the phase space of the molecular complex $(H_3N\text{-}H\text{-}NH_3)^+$.

DOI: 10.1103/PhysRevA.87.042501 PACS number(s): 31.15.xv, 03.65.Xp

I. INTRODUCTION

Ab initio molecular dynamics (AIMD) [1] has become a valid predictive tool in molecular physics, chemistry, and biology thanks to the availability of highly efficient electronic structure methods like Kohn-Sham (KS) density functional theory (DFT) [2]. Initially restricted to a single adiabatic state (Born-Oppenheimer dynamics), DFT-based molecular dynamics was recently extended to the nonadiabatic regime [3–5] becoming an important tool for the study of photophysical and photochemical processes. However, the use of *classical* trajectories in mixed quantum-classical approaches [6] (like, for instance, Tully's trajectory surface hopping [7] (TSH), and quantum-classical Liouville dynamics [8]) poses serious limitations to the possibility of describing pure quantum phenomena such as wave-packet bifurcation [9] and interference [8], (de)coherence, and tunneling effects. As an alternative to trajectory-based approaches, quantum dynamics methods use an *in principle* exact treatment of both electronic and nuclear wave functions (see, for example, Refs. [10,11]). The applicability of these methods is, however, hampered by their high computational costs, which limit the number of accessible nuclear degrees of freedom. In addition, these approaches usually require the fitting of the relevant electronic potential energy surfaces (PESs) prior to propagation. Finally, path integral approaches represent a valid alternative for the investigation of quantum effects in molecular simulations. *Ab initio* path integral sampling techniques [12] and their extensions to quasiclassical dynamics [13] (centroid AIMD [14] and ring-polymer AIMD [15]) have been applied with success in the study of hydrogen-bonded liquids and solids at finite temperatures [16].

An alternative formulation of quantum dynamics derived from the trajectory-based solution of the quantum hydrodynamics equations was proposed by Wyatt in 1999 [17]. In this approach named quantum trajectory method (QTM), the nuclear wave packet is split into fluid elements (FEs) that represent volume elements of the configuration space. These are associated with a nuclear quantum amplitude and a phase that describes the time evolution of the FEs according to a Newton-like equation of motion augmented by a quantum potential (QP) [18]. The resulting quantum trajectories become correlated through the QP and can describe all quantum nuclear effects that are missing in classical trajectory-based approaches.

More recently, several multistate variants of the original QTM dynamics have been proposed [18–21], which mainly differ in the way the electronic PESs are described (diabatic versus adiabatic representation). Despite the enormous potential of these nonadiabatic QTM approaches, three main difficulties are limiting their successful application to molecular systems: (i) the lack of reliable electronic structure methods to couple with the on-the-fly propagation of the nuclear amplitude, (ii) the extension of QTM to the full, unconstrained, multidimensional configuration space, and (iii) the instabilities associated with the calculation of the quantum potential. To our knowledge only the approach in Ref. [18], named nonadiabatic Bohmian dynamics (NABDY), is suited for the on-the-fly calculation of all electronic structure properties (PESs, classical and quantum forces [22], and nonadiabatic couplings [5,23–25]) required for the propagation of the quantum trajectories. In NABDY, the nonadiabatic QTM equations are formulated in Cartesian coordinates while DFT and time-dependent density functional theory (TDDFT) are used to solve the electronic structure at each time step. Despite the success of this approach for the description of the quantum dynamics of small molecules, its extension to systems made of more than a few atoms remains questionable due to the difficulties encountered with points (ii) and (iii) above.

In this article, we develop a quantum trajectory approach to perform quantum dynamics in the high-dimensional, unconstrained, phase space of large molecular systems. The main challenge we face is the calculation of the phase space derivatives of the quantum potential and nuclear amplitudes, which are best performed analytically. To this end, we introduce a decomposition of the nuclear wave packet into a sum of Gaussian functions, which are then propagated in time using a set of differential equations derived from quantum hydrodynamics equations. Within this numerical approximation, the phase space derivatives used in the calculation of the quantum potential can be performed analytically providing

*ivano.tavernelli@epfl.ch

 ©2013 American Physical Society

therefore a solution to the instability problem mentioned in point (iii).

The main target of this explorative work is to provide a theoretical framework to describe adiabatic and nonadiabatic quantum dynamics using Bohmian trajectories in phase space. The applications are, however, restricted to the adiabatic case, which well illustrate the theoretical and numerical challenges associated with this type of dynamics and its level of accuracy without introducing additional complications related to nonadiabaticity. The extension to the nonadiabatic case will require further numerical efforts that are beyond the scope of this work.

This paper is organized in the following way. After the derivation of the main working equations, we will first test the dynamics on molecular hydrogen for which we will compute the first vibrational wave function. Finally, we will demonstrate the quality and the efficiency of this approach by studying the proton transfer dynamics in the (54 dimensional) phase space of the molecular complex $(H_3N\text{-}H\text{-}N\,H_3)^+$.

II. TRAJECTORY-BASED QUANTUM DYNAMICS

The starting point of our derivation is the time-dependent Schrödinger equation,

$$\hat{H}_{\rm mol}\Psi_{\rm mol}(\boldsymbol{r},\boldsymbol{R},t) = i\hbar\frac{\partial}{\partial t}\Psi_{\rm mol}(\boldsymbol{r},\boldsymbol{R},t), \tag{1}$$

where $\boldsymbol{R} = (\boldsymbol{R}_1,\boldsymbol{R}_2,\ldots,\boldsymbol{R}_{N_n})$ is the collective vector of the nuclear positions in $\mathbb{R}^{3N_n}$ and $\boldsymbol{r} = (\boldsymbol{r}_1,\boldsymbol{r}_2,\ldots,\boldsymbol{r}_{N_{el}})$ the one of the electrons. In Eq. (1), $\hat{H}_{\rm mol}$ is the molecular Hamiltonian,

$$\begin{aligned}\hat{H}_{\rm mol}(\boldsymbol{r},\boldsymbol{R}) &= -\sum_\alpha \frac{\hbar^2}{2M_\alpha}\nabla_\alpha^2 - \sum_i \frac{\hbar^2}{2m_e}\nabla_i^2 + \sum_{i<j}\frac{e^2}{|\boldsymbol{r}_i-\boldsymbol{r}_j|}\\ &\quad -\sum_{\alpha,i}\frac{e^2Z_\alpha}{|\boldsymbol{R}_\alpha-\boldsymbol{r}_i|} + \sum_{\alpha<\zeta}\frac{e^2Z_\alpha Z_\zeta}{|\boldsymbol{R}_\alpha-\boldsymbol{R}_\zeta|}\\ &\equiv -\sum_\alpha\frac{\hbar^2}{2M_\alpha}\nabla_\alpha^2 + \sum_{\alpha<\zeta}\frac{e^2Z_\alpha Z_\zeta}{|\boldsymbol{R}_\alpha-\boldsymbol{R}_\zeta|} + \hat{\mathcal{H}}_{\rm el}(\boldsymbol{r},\boldsymbol{R}),\end{aligned} \tag{2}$$

and $\Psi_{\rm mol}(\boldsymbol{r},\boldsymbol{R},t)$ the total wave function of the nuclear and electronic degrees of freedom. Here and in the following equations we use e for the electron charge, Z_α for the atomic number of atom α, and ∇_i and ∇_α for $\nabla_{\boldsymbol{r}_i}$ and $\nabla_{\boldsymbol{R}_\alpha}$, respectively. We will derive equations of motion for the nuclear and electronic degrees of freedom using what is known as a trajectory-based approach: The electrons are described at a quantum mechanical level (using DFT and TDDFT), while the nuclear wave packet is discretized into an ensemble of fluid elements (FEs) in the phase space and then propagated along Bohmian quantum (instead of classical) trajectories.

The Born-Oppenheimer MD equations can be derived starting from the Born-Huang representation of the molecular wave function,

$$\Psi_{\rm mol}(\boldsymbol{r},\boldsymbol{R},t) = \sum_{j=0}^{\infty}\Omega_j(\boldsymbol{R},t)\Psi_j(\boldsymbol{r};\boldsymbol{R}). \tag{3}$$

In this equation, $\{\Psi_j(\boldsymbol{r};\boldsymbol{R})\}$ describes a complete set of orthonormal electronic wave function solution of the time-independent Schrödinger equation,

$$\hat{\mathcal{H}}_{\rm el}(\boldsymbol{r};\boldsymbol{R})\Phi_j(\boldsymbol{r};\boldsymbol{R}) = E_{{\rm el},j}(\boldsymbol{R})\Psi_j(\boldsymbol{r};\boldsymbol{R}), \tag{4}$$

with $\langle\Psi_j|\Psi_i\rangle = \delta_{ij}$ and where "; $\boldsymbol{R}$" denotes the parametric dependence of the electronic Schrödinger equation from the position of the atoms. Note that only the nuclear wave function depends explicitly on time, while $\hat{\mathcal{H}}_{\rm el}(\boldsymbol{r};\boldsymbol{R})$ and $\Psi_j(\boldsymbol{r};\boldsymbol{R})$ only depend on t through the implicit time dependence of $\boldsymbol{R}$, $\boldsymbol{R}(t)$.

Inserting Eq. (3) into the time-dependent Schrödinger equation [Eq. (1)] we obtain (after multiplying by $\Psi_k^*(\boldsymbol{r};\boldsymbol{R})$ from the left-hand side and integrating over $d\boldsymbol{r}$)

$$\begin{aligned}i\hbar\frac{\partial}{\partial t}\Omega_k(\boldsymbol{R},t) &= \left[-\sum_\alpha\frac{\hbar^2}{2M_\alpha}\nabla_\alpha^2 + E_{{\rm el},k}(\boldsymbol{R})\right]\Omega_k(\boldsymbol{R},t)\\ &\quad + \sum_l \mathcal{F}_{kl}\Omega_l(\boldsymbol{R},t).\end{aligned} \tag{5}$$

The quantities $\mathcal{F}_{kl}(\boldsymbol{R})$,

$$\begin{aligned}&\mathcal{F}_{kl}(\boldsymbol{R})\\ &= \int d\boldsymbol{r}\ \Psi_k^*(\boldsymbol{r};\boldsymbol{R})\left[-\sum_\alpha\frac{\hbar^2}{2M_\alpha}\nabla_\alpha^2\right]\Psi_l(\boldsymbol{r};\boldsymbol{R})\\ &\quad + \sum_\alpha\frac{1}{M_\alpha}\left\{\int d\boldsymbol{r}\ \Psi_k^*(\boldsymbol{r};\boldsymbol{R})\,[-i\hbar\nabla_\alpha]\,\Psi_l(\boldsymbol{r};\boldsymbol{R})\right\}[-i\hbar\nabla_\alpha],\end{aligned} \tag{6}$$

are the *nonadiabatic couplings*, with a contribution from the nuclear kinetic energy operator and a second from the momentum operator.

Using the polar representation of the nuclear amplitude $\Omega_j(\boldsymbol{R},t)$,

$$\Omega_j(\boldsymbol{R},t) = A_j(\boldsymbol{R},t)\exp\left[\frac{i}{\hbar}S_j(\boldsymbol{R},t)\right], \tag{7}$$

we obtain the following equations for the phase and the amplitude (both real):

$$\begin{aligned}&\frac{\partial}{\partial t}S_j(\boldsymbol{R},t)\\ &= \frac{\hbar^2}{2}\sum_\alpha M_\alpha^{-1}\frac{\nabla_\alpha^2 A_j(\boldsymbol{R},t)}{A_j(\boldsymbol{R},t)}\\ &\quad -\frac{1}{2}\sum_\alpha M_\alpha^{-1}[\nabla_\alpha S_j(\boldsymbol{R},t)]^2\\ &\quad -\sum_i H_{ji}(\boldsymbol{R})A_{i/j}(\boldsymbol{R},t)\mathrm{Re}\left[e^{[\frac{i}{\hbar}S_{i-j}(\boldsymbol{R},t)]}\right]\\ &\quad -\frac{\hbar^2}{2}\sum_{\alpha i} M_\alpha^{-1}D_{ji}^\alpha(\boldsymbol{R})A_{i/j}(\boldsymbol{R},t)\mathrm{Re}\left[e^{[\frac{i}{\hbar}S_{i-j}(\boldsymbol{R},t)]}\right]\\ &\quad +\hbar^2\sum_{\alpha,i\neq j} M_\alpha^{-1}\mathbf{d}_{ji}^\alpha\frac{\nabla_\alpha A_i(\boldsymbol{R},t)}{A_j(\boldsymbol{R},t)}\mathrm{Re}\left[e^{[\frac{i}{\hbar}S_{i-j}(\boldsymbol{R},t)]}\right]\\ &\quad -\hbar\sum_{\alpha,i\neq j} M_\alpha^{-1}\mathbf{d}_{ji}^\alpha A_{i/j}(\boldsymbol{R},t)\nabla_\alpha S_i(\boldsymbol{R},t)\mathrm{Im}\left[e^{[\frac{i}{\hbar}S_{i-j}(\boldsymbol{R},t)]}\right],\end{aligned} \tag{8}$$

$$
\begin{aligned}
&\hbar\frac{\partial}{\partial t}A_j(\boldsymbol{R},t)\\
&\quad=-\hbar\sum_\alpha M_\alpha^{-1}\nabla_\alpha A_j(\boldsymbol{R},t)\nabla_\alpha S_j(\boldsymbol{R},t)\\
&\quad-\frac{\hbar}{2}\sum_\alpha M_\alpha^{-1}A_j(\boldsymbol{R},t)\nabla_\alpha^2 S_j(\boldsymbol{R},t)\\
&\quad+\sum_i H_{ji}(\boldsymbol{R})A_i(\boldsymbol{R},t)\mathrm{Im}\left[e^{[\frac{i}{\hbar}S_{i-j}(\boldsymbol{R},t)]}\right]\\
&\quad+\frac{\hbar^2}{2}\sum_{\alpha i} M_\alpha^{-1}D_{ji}^\alpha(\boldsymbol{R})A_i(\boldsymbol{R},t)\mathrm{Im}\left[e^{[\frac{i}{\hbar}S_{i-j}(\boldsymbol{R},t)]}\right]\\
&\quad-\hbar^2\sum_{\alpha,i\neq j} M_\alpha^{-1}\mathbf{d}_{ji}^\alpha\nabla_\alpha A_i(\boldsymbol{R},t)\mathrm{Im}\left[e^{[\frac{i}{\hbar}S_{i-j}(\boldsymbol{R},t)]}\right]\\
&\quad-\hbar\sum_{\alpha,i\neq j} M_\alpha^{-1}\mathbf{d}_{ji}^\alpha A_i(\boldsymbol{R},t)\nabla_\alpha S_i(\boldsymbol{R},t)\mathrm{Re}\left[e^{[\frac{i}{\hbar}S_{i-j}(\boldsymbol{R},t)]}\right],
\end{aligned}
\tag{9}
$$

where $A_{i/j}(\boldsymbol{R},t)=\frac{A_i(\boldsymbol{R},t)}{A_j(\boldsymbol{R},t)}$, $S_{i-j}(\boldsymbol{R},t)=S_i(\boldsymbol{R},t)-S_j(\boldsymbol{R},t)$, and

$$
D_{ji}^\alpha=-\int d\boldsymbol{r}\ \Psi_j^*(\boldsymbol{r};\boldsymbol{R})\left[\nabla_\alpha^2\Psi_i(\boldsymbol{r};\boldsymbol{R})\right], \tag{10}
$$

$$
\boldsymbol{d}_{ji}^\alpha=\int d\boldsymbol{r}\ \Psi_j^*(\boldsymbol{r};\boldsymbol{R})\left[\nabla_\alpha\Psi_i(\boldsymbol{r};\boldsymbol{R})\right], \tag{11}
$$

$$
H_{ji}(\boldsymbol{R})=\int d\boldsymbol{r}\ \Psi_j^*(\boldsymbol{r};\boldsymbol{R})\hat{\mathcal{H}}_{el}\Psi_i(\boldsymbol{r};\boldsymbol{R})=\delta_{ji}E_i. \tag{12}
$$

In Eqs. (8) and (9) Re and Im are the symbols for the real and imaginary parts, respectively.

The differential equation for the phase, Eq. (8), can be interpreted as the Hamilton-Jacobi dynamics of a system governed by the action $S_j(\boldsymbol{R},t)$ on the j^{th} PES. Within this formalism, we can solve Eq. (8) by means of its characteristics, which correspond to trajectories in the phase space [26]. Without loss of generality, we restrict the following analysis to two surfaces. Multiplying Eq. (8) from the left by $(-\nabla_{\boldsymbol{R}_\beta})$ we get

$$
\begin{aligned}
\nabla_\beta\frac{\partial S_1(\boldsymbol{R},t)}{\partial t}&=-\nabla_\beta\left(-\frac{\hbar^2}{2}\sum_\alpha M_\alpha^{-1}\frac{\nabla_\alpha^2 A_1(\boldsymbol{R},t)}{A_1(\boldsymbol{R},t)}\right)-\nabla_\beta\frac{1}{2}\sum_\alpha M_\alpha^{-1}[\nabla_\alpha S_1(\boldsymbol{R},t)]^2-\nabla_\beta H_{11}(\boldsymbol{R})\\
&-\nabla_\beta\frac{\hbar^2}{2}\sum_{\alpha i} M_\alpha^{-1}D_{12}^\alpha(t)A_{2/1}(\boldsymbol{R},t)\mathrm{Re}\left[e^{[\frac{i}{\hbar}S_{2-1}(\boldsymbol{R},t)]}\right]+\nabla_\beta\hbar^2\sum_\alpha M_\alpha^{-1}\mathbf{d}_{12}^\alpha(t)\frac{\nabla_\alpha A_2(\boldsymbol{R},t)}{A_1(\boldsymbol{R},t)}\mathrm{Re}\left[e^{[\frac{i}{\hbar}S_{2-1}(\boldsymbol{R},t)]}\right]\\
&-\nabla_\beta\hbar\sum_\alpha M_\alpha^{-1}\mathbf{d}_{12}^\alpha(t)A_{2/1}(\boldsymbol{R},t)\nabla_\alpha S_2(\boldsymbol{R},t)\mathrm{Im}\left[e^{[\frac{i}{\hbar}(S_{2-1}(\boldsymbol{R},t)]}\right],
\end{aligned}
\tag{13}
$$

in the adiabatic representation of the electronic PESs, $H_{ij}=0$ $(i\neq j)$. The gradient ∇_β acts in the $\mathbb{R}^3$ space of the nucleus β, and N_n equivalent equations can be written for each nucleus. A similar equation can be derived for $S_2(\boldsymbol{R},t)$.

The second term on the right-hand side of Eq. (13) can be interpreted as a kinetic term and can be rewritten in the following way:

$$
\begin{aligned}
&\nabla_\beta\frac{1}{2}\sum_\alpha M_\alpha^{-1}[\nabla_\alpha S_1(\boldsymbol{R},t)]^2\\
&\quad=\frac{1}{2}\sum_\alpha M_\alpha^{-1}\nabla_\beta[\nabla_\alpha S_1(\boldsymbol{R},t)]^2=\sum_\alpha M_\alpha^{-1}\nabla_\alpha S_1(\boldsymbol{R},t)\nabla_\beta\nabla_\alpha S_1(\boldsymbol{R},t)=\sum_\alpha M_\alpha^{-1}\nabla_\alpha S_1(\boldsymbol{R},t)\nabla_\alpha\nabla_\beta S_1(\boldsymbol{R},t).
\end{aligned}
\tag{14}
$$

Rearranging Eq. (13) we obtain

$$
\left[\frac{\partial}{\partial t}+\sum_\alpha M_\alpha^{-1}\nabla_\alpha S_1(\boldsymbol{R},t)\nabla_\alpha\right]\nabla_\beta S_1(\boldsymbol{R},t)=-\nabla_\beta[Q_1(\boldsymbol{R},t)+H_{11}(\boldsymbol{R})+d_{[12]}(\boldsymbol{R},t)+D_{[12]}(\boldsymbol{R},t)], \tag{15}
$$

with

$$
\begin{aligned}
Q_1(\boldsymbol{R},t)&=-\frac{\hbar^2}{2}\sum_\alpha M_\alpha^{-1}\frac{\nabla_\alpha^2 A_1(\boldsymbol{R},t)}{A_1(\boldsymbol{R},t)},\\
d_{12}(\boldsymbol{R},t)&=\hbar^2\sum_\alpha M_\alpha^{-1}\mathbf{d}_{12}^\alpha(t)\frac{\nabla_\alpha A_2(\boldsymbol{R},t)}{A_1(\boldsymbol{R},t)}\mathrm{Re}\left[e^{[\frac{i}{\hbar}S_{2-1}(\boldsymbol{R},t)]}\right]-\hbar\sum_\alpha M_\alpha^{-1}\mathbf{d}_{12}^\alpha(t)A_{2/1}(\boldsymbol{R},t)\nabla_\alpha S_2(\boldsymbol{R},t)\mathrm{Im}\left[e^{[\frac{i}{\hbar}S_{2-1}(\boldsymbol{R},t)]}\right],\\
D_{12}(\boldsymbol{R},t)&=\frac{\hbar^2}{2}\sum_{\alpha i} M_\alpha^{-1}D_{12}^\alpha(t)A_{2/1}(\boldsymbol{R},t)\mathrm{Re}\left[e^{[\frac{i}{\hbar}S_{2-1}(\boldsymbol{R},t)]}\right].
\end{aligned}
\tag{16}
$$

Finally, using $\nabla_\beta S_1(\boldsymbol{R},t)/M_\beta=\dot{\boldsymbol{R}}_{\beta,1}$ and the definition for the derivative in the Lagrangian frame,

$$
\frac{\partial}{\partial t}+\sum_\alpha M_\alpha^{-1}\nabla_\alpha S_1(\boldsymbol{R},t)\nabla_\alpha\equiv\frac{d}{dt}, \tag{17}
$$

we obtain the Newton-like equation for the characteristics (or trajectories) associated with the partial differential equation Eq. (15),

$$M_\beta \frac{d}{dt}\dot{\boldsymbol{R}}_{\beta,1}(t) = -\nabla_\beta \left[Q_1(\boldsymbol{R}(t),t) + H_{11}(\boldsymbol{R}(t)) + d_{12}(\boldsymbol{R}(t),t) + D_{12}(\boldsymbol{R}(t),t) \right], \tag{18}$$

which drives the time evolution of the fluid elements in the configuration space. In the same moving frame, the time evolution of the amplitudes becomes [27]

$$\begin{aligned}\hbar \frac{d}{dt} A_j(\boldsymbol{R}(t),t) = &-\frac{\hbar}{2}\sum_\alpha M_\alpha^{-1} A_j(\boldsymbol{R}(t),t)\nabla_\alpha^2 S_j(\boldsymbol{R}(t)) + \sum_i H_{ji}(\boldsymbol{R}(t)) A_i(\boldsymbol{R}(t),t)\mathrm{Im}\left[e^{\left[\frac{i}{\hbar}S_{i-j}(\boldsymbol{R}(t))\right]}\right] \\ &+\frac{\hbar^2}{2}\sum_{\alpha i} M_\alpha^{-1} D_{ji}^\alpha(\boldsymbol{R}(t)) A_i(\boldsymbol{R}(t),t)\mathrm{Im}\left[e^{\left[\frac{i}{\hbar}S_{i-j}(\boldsymbol{R}(t))\right]}\right] - \hbar^2 \sum_{\alpha, i\neq j} M_\alpha^{-1}\mathbf{d}_{ji}^\alpha \nabla_\alpha A_i(\boldsymbol{R}(t),t)\mathrm{Im}\left[e^{\left[\frac{i}{\hbar}S_{i-j}(\boldsymbol{R}(t))\right]}\right] \\ &-\hbar \sum_{\alpha, i\neq j} M_\alpha^{-1}\mathbf{d}_{ji}^\alpha A_i(\boldsymbol{R}(t),t)\nabla_\alpha S_i(\boldsymbol{R}(t))\mathrm{Re}\left[e^{\left[\frac{i}{\hbar}S_{i-j}(\boldsymbol{R}(t))\right]}\right].\end{aligned} \tag{19}$$

III. QUANTUM DYNAMICS IN THE PHASE SPACE: THE GAUSSIAN EXPANSION

We start by approximating the total nuclear amplitude with the product:

$$\begin{aligned}&A(\boldsymbol{R}_1(t),\boldsymbol{R}_2(t),\boldsymbol{R}_3(t),\ldots,\boldsymbol{R}_N(t),t) \\ &\quad = \Phi_1(\boldsymbol{R}_1(t),t)\Phi_2(\boldsymbol{R}_2(t),t)\Phi_3(\boldsymbol{R}_3(t),t)\ldots\Phi_N(\boldsymbol{R}_N(t),t),\end{aligned} \tag{20}$$

where $\Phi_\alpha(\boldsymbol{R}_\alpha(t),t)$ is given by a sum of Gaussians centered at $\boldsymbol{R}_\alpha^{(i)}(t) \in \mathbb{R}^3$,

$$\begin{aligned}\Phi_\alpha(\mathbf{R}_\alpha(t),t) &= \sum_{i=1}^M \tilde{\phi}_\alpha^{(i)}\left(\boldsymbol{R}_\alpha(t) - \boldsymbol{R}_\alpha^{(i)}(t); a_\alpha^{(i)}(t),\sigma_\alpha^{(i)}(t)\right) \\ &= \sum_{i=1}^M \phi_\alpha^{(i)}\left(\boldsymbol{R}_\alpha(t); \boldsymbol{R}_\alpha^{(i)}(t),a_\alpha^{(i)}(t),\sigma_\alpha^{(i)}(t)\right),\end{aligned} \tag{21}$$

and

$$\begin{aligned}&\phi_\alpha^{(i)}\left(\boldsymbol{R}_\alpha(t); \boldsymbol{R}_\alpha^{(i)}(t),a_\alpha^{(i)}(t),\sigma_\alpha^{(i)}(t)\right) \\ &\quad = \frac{a_\alpha^{(i)}(t)}{(2\pi)^{3/2}\left(\sigma_\alpha^{(i)}(t)\right)^3} e^{-\frac{(\boldsymbol{R}_\alpha(t)-\boldsymbol{R}_\alpha^{(i)}(t))^2}{2(\sigma_\alpha^{(i)}(t))^2}} \\ &\quad = \frac{a_\alpha^{(i)}(t)}{\mathcal{N}_\alpha^{(i)}(t)} e^{-\frac{(\boldsymbol{R}_\alpha(t)-\boldsymbol{R}_\alpha^{(i)}(t))^2}{2(\sigma_\alpha^{(i)}(t))^2}}.\end{aligned} \tag{22}$$

The solution of Eq. (19) with the product amplitude given in Eqs. (21) and (22) is still computationally very unpractical. Therefore, we tentatively propose a dynamics in which the centers of the Gaussians follow the time evolution of the characteristics of Eq. (15), i.e., Eq. (18), while the amplitudes of the Gaussians obey Eq. (19). This approach can be formalized using a (coarsed-grained) configuration-space representation of the amplitude [28,29]:

$$A(\boldsymbol{R},t) = \prod_\alpha \sum_{i=1}^M A\left(\boldsymbol{R}_\alpha^{(i)},t\right)\delta\left(\boldsymbol{R}_\alpha - \boldsymbol{R}_\alpha^{(i)}\right), \tag{23}$$

where the $\boldsymbol{R}_\alpha^{(i)}$ are uniformly distributed points in the configuration space with associated amplitude $A(\boldsymbol{R}_\alpha^{(i)},t)$ and evolve according to Eq. (18). The residual, explicit, dynamics of $A(\boldsymbol{R},t)$ is described by Eq. (19). For computational purposes, we introduce a broadening of the Dirac-delta function and work with the representation,

$$A(\boldsymbol{R},t) = \prod_\alpha \sum_{i=1}^M A\left(\boldsymbol{R}_\alpha^{(i)},t\right) g_\alpha^{(i)}\left(\boldsymbol{R}_\alpha - \boldsymbol{R}_\alpha^{(i)}\right), \tag{24}$$

where $g_\alpha^{(i)}(\boldsymbol{R}_\alpha - \boldsymbol{R}_\alpha^{(i)})$ stays for a Gaussian of the form given in Eq. (22) (that gives a Dirac delta function in the limit of $\sigma_{\alpha^{(i)}}$ going to zero), and the centers of the Gaussians, $\boldsymbol{R}_\alpha^{(i)}$, evolve—once more—along the characteristics of Eq. (15). The Gaussians appearing in Eq. (24) have nothing in common with the Gaussians wave packets used in previous works (see, for instance, Ref. [30]) and are not individual solutions of the original time-dependent Schrödinger equation, but they mainly serve as support for the amplitude dynamics given in Eq. (19).

According to the factorizability of the many-body wave functions, the Ansatz in Eq. (20) implies physical (and statistical) independence of all nuclei [31]. In the following, the particle statistics is neglected because, in the most general case, molecules are made of distinguishable atom types. In addition, the statistics is unimportant as far as the thermal wavelength of the particles (with mass M) $\lambda_T = \sqrt{\hbar^2/(2\pi M k_B T)}$ is smaller than the interparticle distance that is roughly proportional to the inverse cube root of the density, $d \sim \rho^{-1/3}$. As a consequence, for temperatures well above the degeneracy temperature $T_d = \rho^{2/3}\hbar^2/(2\pi M k_B T)$ particles can safely be considered distinguishable (Bolzmannions). A generalization of the Ansatz in Eq. (20) is possible but its investigation is beyond the purpose of this article.

It is important to stress that while the nuclear quantization is initially done atom-wise, the *fundamental units of the dynamics* are the phase space fluid elements [FEs with coordinates $(\boldsymbol{R}_1^{(i)},\boldsymbol{R}_2^{(i)},\ldots,\boldsymbol{R}_N^{(i)}) \in \mathbb{R}^{3N}$] associated with the arrays of amplitudes $(a_1^{(i)},a_2^{(i)},\ldots,a_N^{(i)})$, each value $a_\alpha^{(i)}$ corresponding to a Gaussian amplitude linked to a different atom α in the system [according to Eq. (21)]. When analyzed in terms of the FEs, the total nuclear amplitude $\Phi(\boldsymbol{R}) = \sum_i \Phi_i^{FE}(\boldsymbol{R}_1^{(i)},\boldsymbol{R}_2^{(i)},\ldots,\boldsymbol{R}_N^{(i)})$ is no longer a simple product of amplitudes associated with the different fluid elements [32] and therefore it naturally includes correlation [as revealed in the final result for the dynamics of the Gaussian amplitudes in Eq. (39), where the sum over all atoms on the right-hand side implies correlation among the FEs]. The change from atomic, $\Phi_\alpha(\boldsymbol{R}_\alpha)$, to fluid element amplitudes, $\Phi_i^{FE}(\boldsymbol{R}_1^{(i)},\boldsymbol{R}_2^{(i)},\ldots,\boldsymbol{R}_N^{(i)})$, is at the same time necessary and crucial to this development because the electronic structure is computed for a whole molecule (represented by a FE in $\mathbb{R}^{3N}$) and not atom-wise (for each atom separately).

The product Ansatz for the nuclear wave function $\Omega(\mathbf{R}(t))$ implies

$$S(\boldsymbol{R}_1(t),\ldots,\boldsymbol{R}_N(t)) = S_1(\boldsymbol{R}_1(t)) + \cdots + S_N(\boldsymbol{R}_N(t)), \quad (25)$$

for the phases.

A. The dynamics of the fluid elements

The following notation will be used throughout the paper: N refers to number of nuclei that are labeled with the letter $\alpha = 1,\ldots,N$; M is the number of Gaussians per nucleus and corresponds to number of quantum trajectories [labeled with (i), with $i = 1,\ldots,M$], and finally $[i]$ are used to label the different electronic states.

The FE trajectories are the characteristics of the differential equations for the phases for given initial conditions $S_{[i]}(\boldsymbol{R}_0^{[i]},t_0)$ on each PES $[i]$ [18]. A trajectory on a PES $[j]$, $\boldsymbol{R}^{(i)[j]}(t)$, is a $3N$ dimensional array with elements $\boldsymbol{R}^{(i)[j]}(t) = \{\boldsymbol{R}_1^{(i)[j]}(t),\ldots,\boldsymbol{R}_\alpha^{(i)[j]}(t),\ldots,\boldsymbol{R}_N^{(i)[j]}(t)\} \in \mathbb{R}^{3\times N}$ evolving according to [18]

$$M_\beta \frac{d}{dt}\dot{\boldsymbol{R}}_\beta^{[i]}(t) = -\nabla_\beta \left[H_{[i]}(\boldsymbol{R}(t)) + Q_{[i]}(\boldsymbol{R}(t)) + \sum_{[j]} d_{[ij]}(\boldsymbol{R}(t) + D_{[ij]}(\boldsymbol{R}(t)) \right]. \quad (26)$$

As discussed above, the dynamics is "restricted" to the centers of the Gaussians with coordinates $\boldsymbol{R}_\alpha^{(i)}(t)$ and, potentially, to their widths.

1. The quantum potential and forces

The evaluation of Eq. (26) requires the calculation of the derivatives of the quantum potential with respect to the nuclear positions [18]. Here and in the following equations we drop the subscripts for the labeling of the surfaces as well as the explicit time dependence of the position vectors $\mathbf{R}_\alpha(t)$. The quantum forces become

$$-\nabla_\beta Q(\boldsymbol{R}) = -\nabla_\beta \left(-\frac{\hbar^2}{2} \sum_\alpha M_\alpha^{-1} \frac{\nabla_\alpha^2 A(\boldsymbol{R},t)}{A(\boldsymbol{R},t)} \right) = \left(\frac{\hbar^2}{2} M_\beta^{-1} \frac{\nabla_\beta \sum_i \nabla_\beta^2 \phi_\beta^{(i)}(\boldsymbol{R}_\beta,t)}{\sum_i \phi_\beta^{(i)}(\boldsymbol{R}_\beta,t)} \right), \quad (27)$$

which gives

$$-\nabla_\beta Q\big(\boldsymbol{R}_\beta^{(l)}\big) = \left(\frac{\hbar^2}{2} M_\beta^{-1} \frac{\nabla_\beta f\, g - f\, \nabla_\beta g}{g^2}\bigg|_{\boldsymbol{R}_\beta \to \boldsymbol{R}_\beta^{(l)}} \right), \quad (28)$$

with

$$g = \sum_i \phi_\beta^{(i)}\big(\boldsymbol{R}_\beta; a_\beta^{(i)}(t), \sigma_\beta^{(i)}(t)\big), \quad (29)$$

$$f = \sum_{k=1}^{M} \frac{a_\beta^{(i)}(t)}{(2\pi)^{3/2}(\sigma_\beta^{(i)}(t))^5} e^{-\frac{(\boldsymbol{R}_\beta - \boldsymbol{R}_\beta^{(k)})^2}{2(\sigma_\beta^{(k)})^2}} \left[3 - \frac{\big(\boldsymbol{R}_\beta - \boldsymbol{R}_\beta^{(k)}\big)^2}{\big(\sigma_\beta^{(k)}\big)^2} \right], \quad (30)$$

and

$$\nabla_\beta f = \sum_{k=1}^{M} \frac{1}{\big(\sigma_\beta^{(i)}\big)^4} \frac{a_\beta^{(i)}(t)}{\mathcal{N}_\beta^{(i)}(t)} e^{-\frac{(\boldsymbol{R}_\beta - \boldsymbol{R}_\beta^{(k)})^2}{2(\sigma_\beta^{(k)})^2}} \times \big(\boldsymbol{R}_\beta - \boldsymbol{R}_\beta^{(k)}\big) \left[\frac{1}{\big(\sigma_\beta^{(k)}\big)^2} \big(\boldsymbol{R}_\beta - \boldsymbol{R}_\beta^{(k)}\big)^2 - 5 \right], \quad (31)$$

$$\nabla_\beta g = \sum_{k=1}^{M} \frac{-1}{\big(\sigma_\beta^{(k)}\big)^2} \frac{a_\beta^{(k)}(t)}{\mathcal{N}_\beta^{(k)}(t)} e^{-\frac{(\boldsymbol{R}_\beta - \boldsymbol{R}_\beta^{(k)})^2}{2(\sigma_\beta^{(k)})^2}} \big(\boldsymbol{R}_\beta - \boldsymbol{R}_\beta^{(k)}\big). \quad (32)$$

B. Time evolution of the amplitudes

Using the Gaussian expansion in Eq. (20), the differential equation for the amplitude on surface $[j]$, $A_{[j]}$, becomes

$$\sum_\alpha \dot{\Phi}_\alpha^{[j]}(\boldsymbol{R}_\alpha,t) \prod_{\beta\neq\alpha} \Phi_\beta^{[j]}(\boldsymbol{R}_\beta,t) = -\sum_\alpha \frac{1}{2M_\alpha} \left(\prod_\beta \Phi_\beta^{[j]}(\boldsymbol{R}_\beta,t) \right) \nabla_\alpha^2 S_{[j]}(\boldsymbol{R}) + \frac{\hbar^2}{2} \sum_{\alpha,[i]} \frac{1}{M_\alpha} D_{[ji]}^\alpha(t) \left(\prod_\beta \Phi_\beta^{[i]}(\boldsymbol{R}_\beta,t) \right) \mathrm{Im}\big[e^{\mathrm{i}\frac{i}{\hbar}S_{i-j}(\boldsymbol{R}(t))}\big]$$

$$-\hbar \sum_{\alpha,[i]\neq[j]} \frac{1}{M_\alpha} \mathbf{d}^{\alpha}_{[ji]}(t) \left(\prod_{\beta\neq\alpha} \Phi^{[i]}_{\beta}(\boldsymbol{R}_\beta,t) \right) \nabla_\alpha \Phi^{[i]}_{\alpha}(\boldsymbol{R}_\alpha,t) \mathrm{Im}\left[e^{[\frac{i}{\hbar} S_{[i-j]}(\boldsymbol{R})]} \right]$$

$$- \sum_{\alpha,[i]\neq j} \frac{1}{M_\alpha} \mathbf{d}^{\alpha}_{[ji]}(t) \left(\prod_{\beta} \Phi^{[i]}_{\beta}(\boldsymbol{R}_\beta,t) \right) \nabla_\alpha S_{[i]}(\boldsymbol{R}) \mathrm{Re}\left[e^{[\frac{i}{\hbar} S_{[i-j]}(\boldsymbol{R})]} \right]. \tag{33}$$

Applying the identities,

$$\int d\boldsymbol{R}_\alpha \Phi^2_\alpha(\boldsymbol{R}_\alpha) = 1, \quad \int d\boldsymbol{R}_\alpha \nabla_\alpha \Phi_\alpha(\boldsymbol{R}_\alpha) = 0, \quad \int d\boldsymbol{R}_\alpha \Phi_\alpha(\boldsymbol{R}_\alpha) \dot{\Phi}_\alpha(\boldsymbol{R}_\alpha) = 0,$$

we achieve separation by first multiplying Eq. (33) by $\prod_{\beta\neq\alpha} \Phi^{[j]}_\beta(\boldsymbol{R}_\beta,t)$ and then integrating over $\prod_{\beta\neq\alpha} d\boldsymbol{R}_\beta$,

$$\begin{aligned}
\dot{\Phi}^{[j]}_\alpha(\boldsymbol{R}_\alpha,t) = &-\frac{1}{2M_\alpha} \Phi^{[j]}_\alpha(\boldsymbol{R}_\alpha,t) \nabla^2_\alpha S_{[j]}(\boldsymbol{R}) - \Phi^{[j]}_\alpha(\boldsymbol{R}_\alpha,t) \sum_{\beta\neq\alpha} \frac{1}{2M_\beta} \left(\Phi^{[j]}_\beta(\boldsymbol{R}),t \right)^2 \nabla^2_\beta S_{[j]}(\boldsymbol{R}) \\
&+ \frac{\hbar^2}{2} \sum_{[i]} \Phi^{[i]}_\alpha(\boldsymbol{R}_\alpha,t) \left(\sum_\beta \frac{1}{M_\beta} D^{\beta}_{[ji]} \right) [s_\alpha G^c(0) + c_\alpha G^s(0)] \\
&- \hbar \sum_{[i]\neq[j]} \left[\frac{1}{M_\alpha} \mathbf{d}^{\alpha}_{[ji]} \nabla_\alpha \Phi^{[i]}_\alpha(\boldsymbol{R}_\alpha,t) [s_\alpha G^c(0) + c_\alpha G^s(0)] + \sum_{\beta\neq\alpha} \frac{1}{M_\beta} \mathbf{d}^{\beta}_{[ji]} \Phi^{[i]}_\alpha(\boldsymbol{R}_\alpha,t) (s_\alpha F^c + c_\alpha F^s) \right] \\
&- \sum_{[i]\neq[j]} \Phi^{[i]}_\alpha(\boldsymbol{R}_\alpha,t) \left[\frac{1}{M_\alpha} \mathbf{d}^{\beta}_{[ji]} \nabla_\beta S^{[i]}_\alpha(\boldsymbol{R}_\alpha) [c_\alpha G^c(0) - s_\alpha G^s(0)] - c_\alpha \sum_{\beta\neq\alpha} \frac{1}{M_\beta} \mathbf{d}^{\beta}_{[ji]} G^c(1) - s_\alpha \sum_{\beta\neq\alpha} \frac{1}{M_\beta} \mathbf{d}^{\beta}_{[ji]} G^s(1) \right],
\end{aligned} \tag{34}$$

where

$$\begin{aligned}
c_\alpha &= \cos\left(\frac{1}{\hbar} \left(S^{[i]}_\alpha - S^{[j]}_\alpha \right) \right), \quad s_\alpha = \sin\left(\frac{1}{\hbar} \left(S^{[i]}_\alpha - S^{[j]}_\alpha \right) \right), \\
G^c(a) &= \int \left(\prod_{\gamma\neq\alpha} d\boldsymbol{R}_\gamma \left(\Phi^{[i]}_\gamma \Phi^{[j]}_\gamma \right) \right) \left(\nabla_\beta S^{[i]}_\beta \right)^a \cos\left(\sum_{\gamma\neq\alpha} \frac{i}{\hbar} \left(S^{[i]}_\gamma - S^{[j]}_\gamma \right) \right), \\
G^s(a) &= \int \left(\prod_{\gamma\neq\alpha} d\boldsymbol{R}_\gamma \left(\Phi^{[i]}_\gamma \Phi^{[j]}_\gamma \right) \right) \left(\nabla_\beta S^{[i]}_\beta \right)^a \sin\left(\sum_{\gamma\neq\alpha} \frac{i}{\hbar} \left(S^{[i]}_\gamma - S^{[j]}_\gamma \right) \right), \\
F^c &= \int \left(\prod_{\gamma\neq\alpha} d\boldsymbol{R}_\gamma \right) \left(\prod_{\gamma\neq\alpha,\beta} \Phi^{[i]}_\gamma \Phi^{[j]}_\gamma \right) \left(\nabla_\beta \Phi^{[i]}_\beta \right) \Phi^{[j]}_\beta \cos\left(\sum_{\gamma\neq\alpha} \frac{i}{\hbar} \left(S^{[i]}_\gamma - S^{[j]}_{\gamma,} \right) \right), \\
F^s &= \int \left(\prod_{\gamma\neq\alpha} d\boldsymbol{R}_\gamma \right) \left(\prod_{\gamma\neq\alpha,\beta} \Phi^{[i]}_\gamma \Phi^{[j]}_\gamma \right) \left(\nabla_\beta \Phi^{[i]}_\beta \right) \Phi^{[j]}_\beta \sin\left(\sum_{\gamma\neq\alpha} \frac{i}{\hbar} \left(S^{[i]}_\gamma - S^{[j]}_\gamma \right) \right).
\end{aligned}$$

The time dependence of $A(\boldsymbol{R})$ comes from the time evolution of the fluid elements $\boldsymbol{R}^{(i)}_\alpha$ (which is taken into account by the evolution of the trajectory) and from the time evolution of the Gaussian amplitudes $a^{(i)}_\alpha$ and widths $\sigma^{(i)}_\alpha$.

Equation (33) describes the nonadiabatic time evolution of the Gaussian nuclear amplitudes associated with the different nuclei α and PESs $[j]$. In the following, we restrict our analysis to the adiabatic case setting $\mathbf{d}^{\alpha}_{[ji]} = D^{\alpha}_{[ji]} = 0$. In addition, in order to simplify the dynamics, we will introduce the frozen Gaussians approximation for which $\dot{\sigma}^{(i)}_\alpha(t) = 0$. Within these

approximations, Eq. (33) becomes

$$\sum_k \frac{\dot{a}_\alpha^{(k)[j]}(t)}{\sqrt{2\pi}} e^{-\frac{(\boldsymbol{R}_\alpha-\boldsymbol{R}_\alpha^{(k)})^2}{2(\sigma_\alpha^{(k)[j]}(t))^2}} = -\sum_k \frac{1}{2M_\alpha}\frac{a_\alpha^{(k)[j]}(t)}{\mathcal{N}_\alpha^{(k)[j]}} e^{-\frac{(\boldsymbol{R}_\alpha-\boldsymbol{R}_\alpha^{(k)})^2}{2(\sigma_\alpha^{(k)[j]}(t))^2}} \nabla_\alpha^2 S_{[j]}(\boldsymbol{R}) - \left(\sum_k \frac{a_\alpha^{(k)[j]}(t)}{\mathcal{N}_\alpha^{(k)[j]}} e^{-\frac{(\boldsymbol{R}_\alpha-\boldsymbol{R}_\alpha^{(k)})^2}{2(\sigma_\alpha^{(k)[j]}(t))^2}}\right) \sum_{\beta\neq\alpha} \frac{1}{2M_\beta} \left(\sum_k \frac{a_\beta^{(k)[j]}(t)}{\mathcal{N}_\beta^{(k)[j]}} e^{-\frac{(\boldsymbol{R}_\beta-\boldsymbol{R}_\beta^{(k)})^2}{2(\sigma_\beta^{(k)[j]}(t))^2}}\right)^2 \nabla_\beta^2 S_{[j]}(\boldsymbol{R}). \quad (35)$$

The time evolution of the amplitudes $a_\alpha^{(k)[j]}$ is obtained integrating over $\boldsymbol{R}_\alpha$ in Eq. (35). This leads to the following expressions for the different terms in Eq. (35):

(i) Left-hand side:

$$\sum_k \int d\boldsymbol{R}_\alpha \frac{\dot{a}_\alpha^{(k)[j]}(t)}{\mathcal{N}_\alpha^{(k)[j]}} e^{-\frac{(\boldsymbol{R}_\alpha-\boldsymbol{R}_\alpha^{(k)})^2}{2(\sigma_\alpha^{(k)[j]}(t))^2}} = \sum_k \dot{a}_\alpha^{(k)[j]}(t), \quad (36)$$

(ii) First term on the right-hand side:

$$\begin{aligned} &-\sum_k \frac{1}{2M_\alpha} \int d\boldsymbol{R}_\alpha \frac{a_\alpha^{(k)[j]}(t)}{\mathcal{N}_\alpha^{(k)[j]}} e^{-\frac{(\boldsymbol{R}_\alpha-\boldsymbol{R}_\alpha^{(k)})^2}{2(\sigma_\alpha^{(k)[j]}(t))^2}} \nabla_\alpha^2 S_{[j]}(\boldsymbol{R}_\alpha) \\ &= -\frac{1}{2M_\alpha} \sum_k \frac{a_\alpha^{(k)[j]}(t)}{\mathcal{N}_\alpha^{(k)[j]}} \int d\boldsymbol{R}_\alpha \left(e^{-\frac{(\boldsymbol{R}_\alpha-\boldsymbol{R}_\alpha^{(k)})^2}{2(\sigma_\alpha^{(k)[j]}(t))^2}}\right) \nabla_\alpha^2 S_{[j]}(\boldsymbol{R}_\alpha) \\ &= -\frac{1}{2M_\alpha} \sum_k \sum_l \frac{a_\alpha^{(k)[j]}(t)}{\mathcal{N}_\alpha^{(k)[j]}} \\ &\times \left(\int d\boldsymbol{R}_\alpha \frac{\left|\boldsymbol{R}_\alpha - \boldsymbol{R}_\alpha^{(l)}\right|^{-2} e^{-\frac{(\boldsymbol{R}_\alpha-\boldsymbol{R}_\alpha^{(k)})^2}{2(\sigma_\alpha^{(k)[j]}(t))^2}}}{\sum_p \left|\boldsymbol{R}_\alpha - \boldsymbol{R}_\alpha^{(p)}\right|^{-2}}\right) \nabla_\alpha^2 S_{[j]}\left(\boldsymbol{R}_\alpha^{(l)}\right) \\ &\equiv -\frac{1}{2M_\alpha} \sum_k \sum_l \frac{a_\alpha^{(k)[j]}(t)}{\mathcal{N}_\alpha^{(k)[j]}} \mathcal{X}_\alpha^{(k,l)} \nabla_\alpha^2 S_{[j]}\left(\boldsymbol{R}_\alpha^{(l)}\right). \end{aligned} \quad (37)$$

We compute the scalar field $\nabla_\alpha^2 S_{[j]}(\boldsymbol{R})$ from the curvature of $S_{[j]}(\boldsymbol{R})$ along the trajectory. The integral over $d\boldsymbol{R}_\alpha$ in the third line is evaluated using a Shepard algorithm [33] with interpolating function r^{-2} and interpolation points $\boldsymbol{R}_\alpha^{(l)}(t)$ corresponding to the configurations sampled by all other trajectories ($l \neq k$) at the same instant of time t.

(iii) Second term on the right-hand side:

$$\begin{aligned} &-\sum_\beta \frac{\sum_k a_\alpha^{(k)}(t)}{2M_\beta} \\ &\times \int d\boldsymbol{R}_\beta \left(\sum_k \frac{a_\beta^{(k)[j]}(t)}{\mathcal{N}_\beta^{(k)[j]}} e^{-\frac{(\boldsymbol{R}_\beta-\boldsymbol{R}_\beta^{(k)})^2}{2(\sigma_\beta^{(k)[j]}(t))^2}}\right)^2 \nabla_\beta^2 S_{[j]}(\boldsymbol{R}_\beta) \\ &= -\sum_\beta \frac{\sum_k a_\alpha^{(k)}(t)}{2M_\beta} \sum_l \int d\boldsymbol{R}_\beta \left(\sum_k \frac{a_\beta^{(k)[j]}(t)}{\mathcal{N}_\beta^{(k)[j]}} e^{-\frac{(\boldsymbol{R}_\beta-\boldsymbol{R}_\beta^{(k)})^2}{2(\sigma_\beta^{(k)[j]}(t))^2}}\right)^2 \\ &\times \frac{\left|\boldsymbol{R}_\beta - \boldsymbol{R}_\beta^{(l)}\right|^{-2}}{\sum_p \left|\boldsymbol{R}_\beta - \boldsymbol{R}_\beta^{(p)}\right|^{-2}} \nabla_\beta^2 S_{[j]}\left(\boldsymbol{R}_\beta^{(l)}\right) \\ &\equiv -\sum_\beta \frac{\sum_k a_\alpha^{(k)}(t)}{2M_\beta} \sum_l \mathcal{W}_\beta^{(l)} \nabla_\beta^2 S_{[j]}\left(\boldsymbol{R}_\beta^{(l)}\right). \end{aligned} \quad (38)$$

As in (ii), a Shepard algorithm is used to perform the integral in $d\boldsymbol{R}_\beta$.

Finally, applying Jones' solution [34] to Eq. (35) we obtain the following set differential equations for the FEs amplitudes (see appendix):

$$\begin{aligned} \dot{a}_\alpha^{(k)}(t) = &-\frac{1}{2M_\alpha} \sum_l \frac{a_\alpha^{(k)}(t)}{\left(\sqrt{2\pi}\sigma_\alpha^{(k)[j]}(t)\right)^3} \mathcal{X}_\alpha^{(k,l)} \nabla_\alpha^2 S\left(\boldsymbol{R}_\alpha^{(l)}\right) \\ &-\sum_\beta \frac{a_\alpha^{(k)}(t)}{2M_\beta} \sum_l \mathcal{W}_\beta^{(l)} \nabla_\beta^2 S_{[j]}\left(\boldsymbol{R}_\beta^{(l)}\right) \\ &-a_\alpha^{(k)}(t)\Omega\left(\left\{a_\alpha^{(l)}(t)\right\}\right). \end{aligned} \quad (39)$$

The last term in Eq. (39) arises from the norm conservation of Φ_α where $\Omega(\{a_\alpha^{(l)}\}) = 1/(\sum_{l=1} F_{a_\alpha^{(l)}} a_\alpha^{(l)})(\sum_{l=1} L_l(\{a_\alpha^{(l)}\}) F_{a_\alpha^{(l)}})$, $L_l(\{a_\alpha^{(l)}\})$ is the sum of the first two terms of the right-hand side of Eq. (39), and $F_{a_\alpha^{(l)}}$ is the partial derivative with respect to $a_\alpha^{(l)}$ of the constraint $F(\{a_\alpha^{(l)}\}) = \int d\boldsymbol{R}_\alpha (\sum_l \phi_\alpha^{(l)})^2 - 1 = 0$ [34].

C. The numerical algorithm

Equation (26) with Eqs. (28) and (39) constitute the set of adiabatic Bohmian dynamics (ABDY) equations used for the numerical implementation of the coupled quantum electron-nuclear dynamics in phase space. The gradients $\nabla_\alpha S(\boldsymbol{R}_\alpha^{(k)})$ correspond to the momenta $\boldsymbol{P}_\alpha^{(k)}$, while the Laplacians $\nabla_\alpha^2 S(\boldsymbol{R}_\alpha^{(k)})$ are obtained from the curvature of the trajectory (k) evaluated at time t. To improve the stability of the algorithm, we introduce a softening of the quantum potential in Eq. (28) by adding a constant γ to the denominator.

In a typical calculation, we start by distributing a set of centers, $\boldsymbol{R}_\alpha^{(k)}$, according to Gaussian distributions centered on each atom α of the system, where the initial geometry is taken from an equilibrated classical run at the desired temperature. The atomic positions sampled in this way are the center of the frozen Gaussians, $\phi_\alpha^{(k)}(\boldsymbol{R}_\alpha, a_\alpha^{(k)})$, used to propagate the nuclear amplitudes, while a molecular FE consists of a collection of atomic coordinates defining a molecule. The classical momenta are then redistributed with a spread $\delta\boldsymbol{P}_\alpha^{(k)} \sim h/\delta\boldsymbol{R}_\alpha^{(k)}$ (where h is the Plank constant). The softening parameter γ is chosen within the range $[10^{-11}, 10^{-9}]$ and the time step is typically set to 0.024 fs (but it is reduced by a factor 10 when a bond between two H atoms is present). The ABDY scheme is implemented in the plane wave DFT-TDDFT code CPMD [35].

IV. APPLICATIONS

To validate ABDY in the adiabatic (ground-state) regime, we compute the vibrational wave function of the hydrogen molecule in its first ground-state vibrational state. In this

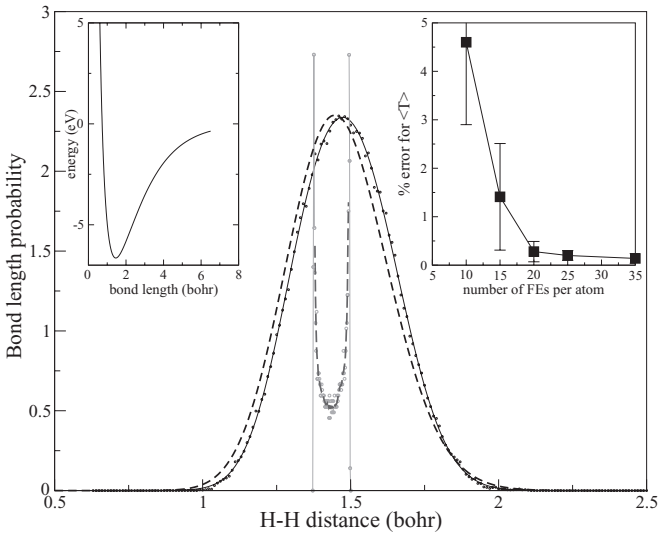

FIG. 1. Ground-state squared vibrational wave function of the hydrogen molecule computed with an ensemble of 20 Bohmian trajectories for a total simulation time of 500 fs (circles); a fit with three Gaussians is also shown (black curve). The ABDY solution is compared with the numerical solution obtained with finite differences (dashed line) and with the (unnormalized) classical bond length distribution (gray dashed curve). The DFT potential curve for H_2 is computed with the PBE functional [36] and a plane-wave cutoff of 50 Ry (see left inset). The right inset reports the percentage error in kinetic energy $\langle \hat{T} \rangle$ as a function of the number of FEs per atom.

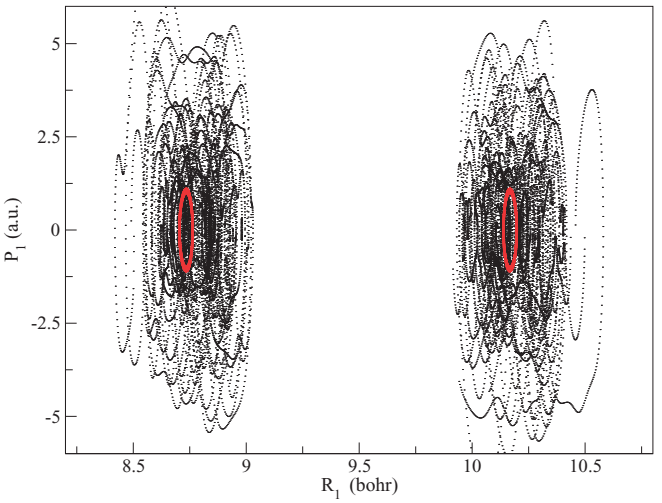

FIG. 2. (Color online) Projection onto the (R_1, P_1) plane of the atomic FE dynamics of the two hydrogen atoms (black dots) compared to the classical trajectories (red circles). The equilibrium position is at $R_1(H_{\alpha=1}) = 8.73$ bohr and $R_1(H_{\alpha=2}) = 10.16$ bohr.

application, each atom is represented by 20 FEs Gaussian distributed around the "classical" atoms placed at a distance of 0.8 Å(roughly the turning point of the classical trajectory at 300 K) with a variance of 0.1 Å. The dynamics is performed with the PBE functional [36] and a plane-wave cutoff of 50 Ry.

Figure 1 shows the results obtained from our dynamics (black line) together with the numerical solution obtained with the finite-differences method (dashed black line) applied to the same DFT-PBE potential, and the classical bond length distribution at ∼300 K (dashed gray line). The agreement between the two quantum calculations is very good with just a deviation of about 1% in the position of the distribution maxima. It is important to mention that in ABDY we quantized the single atoms according to the Ansatz in Eq. (20) and not directly the first bound state of the intramolecular potential. As a consequence, we do not obtain the exact stationary state of the system (with all its implications [37,38]) but, more appropriately, a "quasistationary" state whose time average is reported in Fig. 1. The convergence of the calculation as a function of the number of the atomic FEs is shown in the right inset. Note that the momenta of the FEs can reach higher values than that associated to the FEs center of mass, while the quantum kinetic energy $\langle \hat{T} \rangle$ is in agreement with the reference calculation. Figure 2 reports a two-dimensional cut through the molecular phase space showing the projected position and momenta distributions onto the (R_1, P_1) plane of the two hydrogen atoms (R_1 and P_1 are the first Cartesian coordinate and momentum of each hydrogen atom [39]). By taking the classical limit $Q \to 0$ the FEs will behave as uncorrelated classical systems with an independent time evolution. In this limit case, all atoms defining a FE will therefore follow classical trajectories in the phase space (see red elliptical trajectories in Fig. 2). It is indeed the presence of quantum correlation among the FEs that induces the deviation from the classical behavior and generates the complex (almost chaotic) FE dynamics shown by the black dotted trajectories in Fig. 2. In addition, this correlation is also responsible for the correct quantum distribution of the H_2 bond length (black line in Fig. 1), which in the case of classical dynamics is described by a bimodal distribution with two maxima at the turning points (gray dashed line in Fig. 1). This is an indirect proof of the correct physical nature of the correlation between FEs.

Of particular interest is the use of ABDY in the direct investigation of dynamical properties of molecular systems for which nuclear quantum effects play an important role. In the adiabatic case, the most relevant of such processes is proton transfer (PT). In the following we first compute the PT dynamics of an extra proton placed between two ammonia molecules separated by a fix N to N distance of 2.63 Å, while in a second simulation we will investigate the same PT process in the fully unconstrained phase space of the molecular complex.

The constraint on the N-N distance is imposed to stabilize the system in a reactive configuration with the aim of enhancing the probability of proton transfer within the time scale of our simulation (100 fs). In particular, at this N-N distance the barrier for classical proton transfer is prohibitively high, which gives us the opportunity to study a pure quantum tunneling process. The ABDY dynamics is performed in the 53-dimensional molecular phase space using electronic potential and forces computed on-the-fly using DFT with the PBE functional and a plane-wave cutoff of 70 Ry. Thirty FEs are used for each atom (Fig. 3, upper left panel). During the equilibrating Born-Oppenheimer dynamics with classical nuclei ($t < 0$ in Fig. 3) the shared proton remains linked to the same nitrogen atom and no transfer is observed over a period of more than 10 ps (data not shown). The situation changes when we switch to quantum dynamics at time $t = 0$. In average

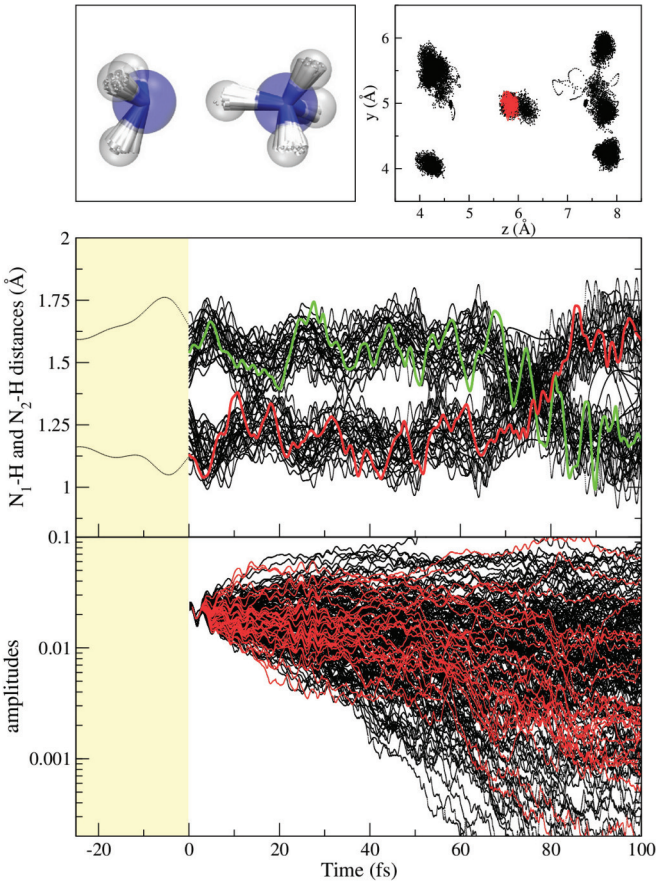

FIG. 3. (Color online) (Upper left panel) Ball-and-stick representation of the $(NH_3)_2$ H^+ system. Thirty FEs per atom are used in the quantum dynamics (small spheres). Large atom-centered vdW spheres are used to wrap up all atomic FEs (blue, nitrogen; white, hydrogen). (Upper right panel) Collection of all FE centers collected along the entire simulation. (Middle panel) Time series of the two N-H distances with the shared proton; ($t < 0$), dynamics with classical nuclei; ($t > 0$), dynamics with quantum trajectories. Two representative paths are shown in color to highlight the transition. (Lower panel) Time series of the Gaussian midpoint amplitudes of the FEs associated with the different hydrogen atoms (black lines). In red is highlighted the dynamics of the 30 FE amplitudes of the "shared" proton.

the two NH distances become shorter and we observe a first PT event within the first 100 fs of quantum dynamics (Fig. 3, middle panel). The upper right panel in Fig. 3 shows the entire set of atomic FE centers collected along the full 0.35-ps-long simulation. The scattering of the FE "clouds" is due to both the quantum spread and the statistical sampling (umbrella motion of the NH_3 units). In red (Fig. 3, upper right panel) are shown the configurations of the central hydrogen atom that are closer to the "acceptor" nitrogen atom on the left; in the stating configuration the same H atom was bonded to the "donor" nitrogen on the right. Finally, in the lower panel of Fig. 3 we report the time series of the amplitudes of all FEs.

A more realistic description of the proton transfer dynamics in this complex is obtained when the constraint on the N-N is released. However, due to the low frequency of the N-N mode an exhaustive sampling of this additional degree of freedom is beyond the reach of the present study and therefore here

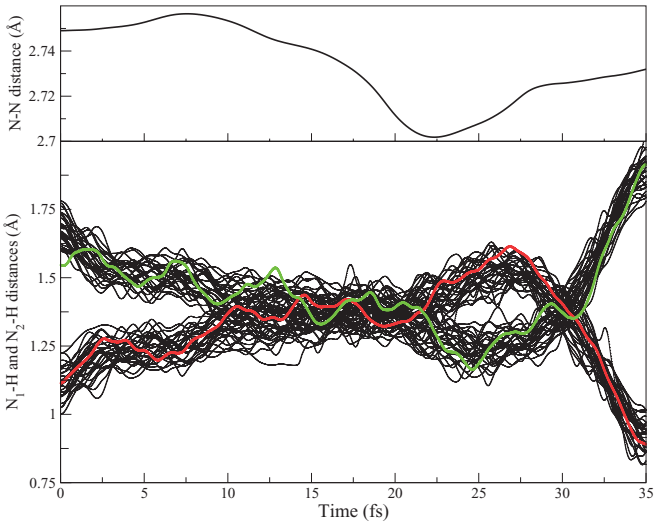

FIG. 4. (Color online) (Upper panel) Time series of the average N-N bond distance for the unconstrained ABDY dynamics of the $(NH_3)_2$ H^+ complex. (Lower panel) Time series of the two N-H distances with the shared proton. Two representative paths are shown in color to highlight the transitions. Three snapshots represented the molecular system at times $t = 0$ (initial configuration), $t = 25$ (after the first proton transfer), and $t = 35$ fs (last frame) are also shown. (Color code as in Fig. 3).

we will only report the dynamics associated to a single N-N vibration period.

The simulation is started by assigning collinear antiparallel velocities to the nitrogen atoms. Figure 4 shows the time evolution of the quantum averaged N-N distance (upper panel) together with the corresponding N-H distances computed for each FE separately (lower panel). We clearly observe a correlation between the N-N distance and the occurrence of a PT event, as far as the NH_3 molecules remain oriented face-to-face as shown in the upper panel of Fig. 3. In addition, this dynamics offers the possibility of investigating the role of other molecular degrees of freedom in the modulation of the PT process. In particular, Fig. 5 shows that the PT in the $(NH_3)_2$ H^+ complex occurs preferentially at large pyramidalization values of the acceptor molecule and for noncollinear N-H bonds (i.e., for N-H-N angles between 150° and 170°). We also observed that this specific choice of the initial velocities induces a rotation of one ammonia molecule with respect to the other making a subsequent PT event less favorable (see inset in Fig. 4, lower panel). It is important to stress that a full rationalization of the PT dynamics in the unconstrained configuration space of $(NH_3)_2$ H^+ will require the collection of many initial conditions, which is beyond the scope of this study.

V. DISCUSSION AND CONCLUSIONS

We have presented a approach to perform quantum dynamics of molecular systems using Bohmian trajectories and electronic structure properties computed *on-the-fly* with DFT. The dynamics is based on the solution by characteristics of the differential equation for the action function in the configuration space. The characteristics are trajectories that

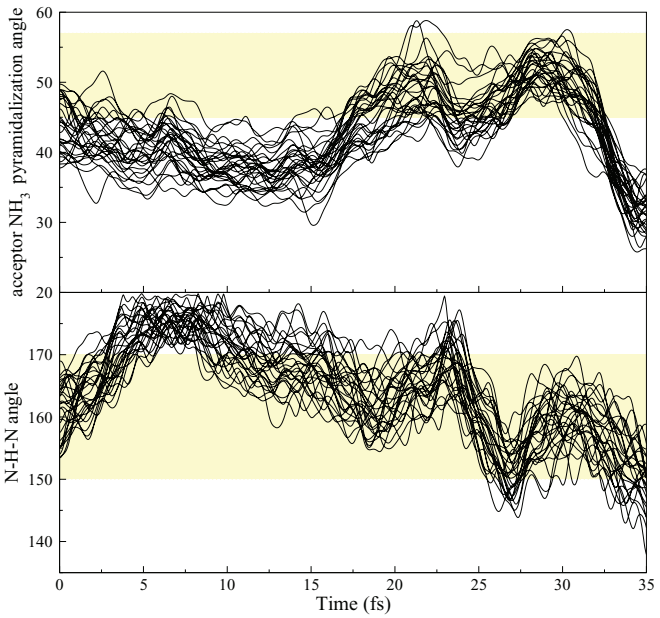

FIG. 5. (Color online) Time series of the pyramidalization angle of the acceptor NH_3 molecule (upper panel) and of the N-H-N angle (lower panel) during 35 fs of unconstrained dynamics of the $(NH_3)_2H^+$ complex.

propagate phase space volume elements (fluid elements) in the quantum hydrodynamic representation of the nuclear dynamics [31,40]. The main challenge in the implementation of this type of dynamics for molecular systems is related to the high dimensionality of the problem, which hampers the use of prepared PESs to guide the nuclear dynamics. To overcome this problem, we have recently developed a nonadiabatic Bohmian dynamics scheme (NABDY) that combines the propagation of quantum trajectories with the on-the-fly calculation of PESs, forces, and nonadiabatic couplings using DFT and TDDFT [18]. Building from this work, we derived an *ab initio*–driven quantum dynamics scheme that can handle molecular systems of any dimension. This is accomplished at the cost of some approximations. The most severe is related to the factorization of the nuclear wave function given in Eq. (20). In fact, this product Ansatz implies physical independence of the different particles, which prevents us from describing entangled, highly correlated nuclear states. However, the molecular FEs remain correlated at all times. While this approximation appears severe in many cases, the corresponding dynamics can still capture important effects related to the quantum nature of constituent subsystems (like quantum dots and light elements in molecules) including nuclear wave-packet splitting, tunneling, and, possibly, nonadiabatic transitions. Additional approximations are introduced for numerical purposes; their effect on the dynamics can in general be tuned through the settings of corresponding control parameters. Those are (i) the number of Gaussian functions used in the representation of the nuclear wave packets, which corresponds to the number of atomic fluid elements (FEs), (ii) the softening of the quantum potential, which produces a smoothening of the forces acting on the FEs and consequently permits the use of larger time steps in the integration of the equations of motion, and (iii) the frozen Gaussian approximation, which imposes the time evolution of Gaussians with constant widths. Most importantly, the use of the Gaussian expansion for the nuclear amplitudes has the enormous beneficial effect of making the calculation of the quantum potential and corresponding forces analytic [Eq. (28)]. This brings further stability into the numerical solution of the quantum dynamics.

While this dynamics (named (adiabatic Bohmian dynamics) is derived for the most general nonadiabatic case, in this work we restricted its implementation and applications to the adiabatic limit. We first applied ABDY to the study of the vibronic wave function of the H_2 molecule, which has the largest quantum effects among all diatomics. The H_2 bond length distribution sampled with the quantum trajectories is in very good agreement with the "exact" solution obtained solving by finite differences the time-independent Schrödinger equation for the same one-dimensional DFT potential (see Fig. 1). In particular, we found that the results already converge with 20 FEs per atom and a softening coefficient $\gamma = 10^{-9}$. The analysis of the trajectories reveals how the sampling of rare classical configurations is achieved; by the action of the quantum potential FEs are accelerated and move into regions of the configuration space that are classically forbidden. However, the FE dynamics has no direct relation to the molecular kinetic energy, which is now computed as the expectation value of the kinetic operator.

Finally, we applied ABDY to the investigation of dynamic nuclear quantum effects in AIMD simulations of molecular systems and in particular to the study of the proton transfer dynamics in the molecular complex $(H_3N\text{-}H\text{-}NH_3)^+$. Initially, the quantum dynamics is performed in the full molecular phase space with the only exception of the N-N distance that is kept fixed at the value of 2.63 Å in order to better compare with the classical dynamics that, being simulated on a longer time scale, would modify substantially this arrangement. We observed that, while the PT does not occur during several *ps* of classical AIMD, it is strongly enhanced when the quantum description of the nuclear dynamics is switched on (Fig. 3). Not surprisingly, the larger quantum effects are observed for the hydrogen atoms, which have the largest spread in configuration space. In a second step, we released the N-N distance constraint and we simulated the PT process starting from collinear antiparallel velocities assigned to the nitrogen atoms. We observe a faster PT dynamics that occurs for short values of the N-N distance. However, other molecular vibrational modes appear to play a role in the process like, for instance, the pyramidalization of the ammonia molecules and the misalignment of the N-H-N triad. As shown in this simple application, ABDY has the potential of emerging as a valuable complementary scheme to path integral techniques for the study of nuclear quantum effects in molecules, liquids, and solids.

Numerically, the ABDY scheme is simple to implement in any DFT-based molecular dynamics code and due to the low level of communication between trajectories it can be efficiently parallelized.

In conclusion, the development presented in this work together with the results of Ref. [18] provide a complete theoretical framework for the implementation of a nonadiabatic MD scheme based on quantum trajectories. In the adiabatic case, ABDY constitutes a valuable approach for

the calculation of nuclear quantum effects in *ab initio*–driven AIMD simulations. Finally, it is worth mentioning that, while the factorization Ansatz of the nuclear wave function considerably simplifies the equations of motion, it is not essential to this development. We are currently working on possible alternative representation of the correlated nuclear wave function, which will open new perspectives in the study of entangled quantum dynamics.

ACKNOWLEDGMENTS

The author acknowledges Giovanni Ciccotti for his precious scientific support, and Basile Curchod and Sara Bonella for their useful comments. COST action CM0702 and Swiss National Science Foundation Grants No. 200020-130082 and No. 200021-137717 are acknowledged for funding.

APPENDIX

The coupled system of (linear) differential equations,

$$\dot{x}_i = L_i(\vec{x}), \tag{A1}$$

with the initial conditions $x_i(0) = x_i^0$ and the constraint,

$$F(\vec{x},t) = c, \tag{A2}$$

can be rewritten as

$$\dot{x}_i = L_i(\vec{x}) - x_i\Omega(\vec{x},t)\,, \tag{A3}$$

where Ω is

$$\Omega(\vec{x},t) = \frac{1}{\sum_{j=1}^{n} F_{x_j} x_j}\left(\sum_{i=1}^{n} L_i(\vec{x})F_{x_i} + F_t\right), \tag{A4}$$

and $F_{x_i} = \partial F/\partial x_i$, and $F_t = \partial F/\partial t$. In addition, when $F(\vec{x})$ is homogeneous of order λ in all its variables, $F(a\vec{x}) = a^\lambda F(\vec{x})$, then

$$\Omega(\vec{x},t) = \frac{1}{\lambda c}\left(\sum_{i=1}^{n} L_i(\vec{x})F_{x_i} + F_t\right). \tag{A5}$$

Proof. From

$$\dot{F}(\vec{x},t) = 0, \tag{A6}$$

one gets

$$\sum_i F_{x_i}\dot{x}_i + F_t = 0, \tag{A7}$$

and inserting Eq. (A3),

$$\sum_i F_{x_i}(L_i(\vec{x}) - x_i\Omega(\vec{x},t)) + F_t = 0 \tag{A8}$$

gives the desired equation for Ω. ■

Algorithm

If $L_i(\vec{x})$ is an homogeneous function on all x_i, then the differential equation with constraint [Eq. (A3)],

$$\dot{x}_i = L_i(\vec{x}) - x_i\Omega(\vec{x},t), \tag{A9}$$

can be recast into the original form,

$$\dot{y}_i = L_i(\vec{y}), \tag{A10}$$

by means of the transformation,

$$x_i(t) = y_i(t)\, e^{-\int_0^t d\tau\Omega(\tau)}. \tag{A11}$$

Proof. Inserting the derivative of Eq. (A11),

$$\dot{x}_i(t) = \dot{y}_i(t)\, f(t) + y_i(-\Omega)f(t), \tag{A12}$$

into the original equation,

$$\dot{x}_i = L_i(\vec{x}) - x_i\Omega(\vec{x},t), \tag{A13}$$

with $f(t) = e^{-\int_0^t d\tau\Omega(\tau)}$, one gets

$$\dot{y}_i = L_i(\vec{x})\frac{1}{f(t)}. \tag{A14}$$

Assuming that $L_i(\vec{x})$ is homogeneous, then [since $\vec{y} = \vec{x}/f(t)$]

$$\dot{y}_i = L_i(\vec{y})\,. \tag{A15}$$

■

Corollary. If $F(\vec{x},t)$ is homogeneous in x_i then

$$\begin{aligned} c &= F(\vec{x},t) \\ &= F(\vec{y}\, f(t),t) \\ &= (f(t))^\lambda F(\vec{y},t). \end{aligned}$$

Therefore,

$$f(t) = \left(\frac{c}{F(\vec{y},t)}\right)^{1/\lambda} \tag{A16}$$

and

$$x_i(t) = y_i(t)\left(\frac{c}{F(\vec{y},t)}\right)^{1/\lambda}. \tag{A17}$$

[1] D. Marx and J. Hutter, in *Modern Methods and Algorithms of Quantum Chemistry*, Vol. 1 of NIC Series (Forschungszentrum Juelich, Juelich, 2000), p. 301.
[2] W. Kohn and L. J. Sham, Phys. Rev. **140**, 1133 (1965).
[3] N. L. Doltsinis and D. Marx, Phys. Rev. Lett. **88**, 166402 (2002).
[4] C. F. Craig, W. R. Duncan, and O. V. Prezhdo, Phys. Rev. Lett. **95**, 163001 (2005).
[5] E. Tapavicza, I. Tavernelli, and U. Rothlisberger, Phys. Rev. Lett. **98**, 023001 (2007).
[6] S. Nielsen, R. Kapral, and G. Ciccotti, J. Chem. Phys. **112**, 6543 (2000).
[7] J. C. Tully, J. Chem. Phys. **93**, 1061 (1990).
[8] I. Horenko, C. Salzmann, B. Schmidt, and C. Schutte, J. Chem. Phys. **117**, 11075 (2002).
[9] Y. Arasaki, K. Takatsuka, K. Wang, and V. McKoy, Phys. Rev. Lett. **90**, 248303 (2003).
[10] H. D. Meyer, U. Manthe, and L. S. Cederbaum, Chem. Phys. Lett. **165**, 73 (1990).

[11] M. Ben-Nun, J. Quenneville, and T. J. Martinez, J. Phys. Chem. A **104**, 5161 (2000).

[12] D. Marx and M. Parrinello, Z. Phys. B **95**, 143 (1994).

[13] M. T. D. Marx and G. Martina, Comp. Phys. Comm. **118**, 166 (1999).

[14] J. Cao and G. Voth, J. Chem. Phys. **99**, 10070 (1996).

[15] B. Braams and D. Manolopoulos, J. Chem. Phys **125**, 124105 (2006).

[16] D. Marx, ChemPhysChem **7**, 1848 (2006).

[17] C. L. Lopreore and R. E. Wyatt, Phys. Rev. Lett. **82**, 5190 (1999).

[18] B. F. E. Curchod, I. Tavernelli, and U. Rothlisberger, PhysChemChemPhys. **13**, 3231 (2011).

[19] R. E. Wyatt, C. L. Lopreore, and G. Parlant, J. Chem. Phys. **114**, 5113 (2001).

[20] C. L. Lopreore and R. E. Wyatt, J. Chem. Phys. **116**, 1228 (2002).

[21] B. Poirier and G. Parlant, J. Phys. Chem. A **111**, 10400 (2007).

[22] J. Hutter, J. Chem. Phys. **118**, 3928 (2003).

[23] I. Tavernelli, E. Tapavicza, and U. Rothlisberger, J. Chem. Phys. **130**, 124107 (2009).

[24] I. Tavernelli, B. F. E. Curchod, and U. Rothlisberger, J. Chem. Phys. **131**, 196101 (2009).

[25] I. Tavernelli, B. F. E. Curchod, A. Laktionov, and U. Rothlisberger, J. Chem. Phys. **133**, 194104 (2010).

[26] V. Arnold, *Mathematical Methods of Classical Mechanics* (Springer-Verlag, Berlin, 1989).

[27] The fact that $dA_j(\boldsymbol{R}(t),t)/dt$ depends on $\nabla^2_\alpha S_j(\boldsymbol{R}(t))$ can induce a dependence of this type in the right-hand side of Eq. (19), which will then make its solution by characteristic questionable. However, despite this potential complication, we did not find so far any instability in the numerical solution of Eq. (18) that could be related to this problem.

[28] Y. L. Klimontovich, *The Statistical Theory of Non-Equilibrium Processes in a Plasma* (MIT Press, Cambridge, 1967).

[29] S. Ichimaru, *Statistical Plasma Physics* (Addison-Wesley, Reading, 1992).

[30] R. Littlejohn, Rev. Phys. **138**, 193 (1986).

[31] P. R. Holland, *The Quantum Theory of Motion–An Account of the de Broglie-Bohm Causal Interpretation of Quantum Mechanics* (Cambridge University Press, Cambridge, 1993).

[32] Consider the case of a diatomic system (like, for instance, H_2) with two Gaussians per atom. Atom-wise, the nuclear amplitude is simply $A(\boldsymbol{R}) = \Phi_1(\boldsymbol{R}_1)\Phi_2(\boldsymbol{R}_2)$, with $\Phi_\alpha(\boldsymbol{R}_\alpha) = \phi^{(1)}_\alpha(\boldsymbol{R}^{(1)}_\alpha) + \phi^{(2)}_\alpha(\boldsymbol{R}^{(2)}_\alpha)$. In the fluid element representation, the same amplitude becomes $A(\boldsymbol{R}) = \phi^{(1)}_1(\boldsymbol{R}^{(1)}_1)\phi^{(1)}_2(\boldsymbol{R}^{(1)}_2) + \phi^{(1)}_1(\boldsymbol{R}^{(1)}_1)\phi^{(2)}_2(\boldsymbol{R}^{(2)}_2) + \phi^{(2)}_1(\boldsymbol{R}^{(2)}_1)\phi^{(2)}_2(\boldsymbol{R}^{(2)}_2) + \phi^{(2)}_1(\boldsymbol{R}^{(2)}_1)\phi^{(1)}_2(\boldsymbol{R}^{(1)}_2)$, where each term is a fluid element (or a "molecule") and the cross-terms describe correlation. More precisely, the correlation between two FEs can be easily evaluated as the difference between the two-body FE density $\rho((\boldsymbol{R}^{(1)}_1,\boldsymbol{R}^{(1)}_2),(\boldsymbol{R}^{(2)}_1,\boldsymbol{R}^{(2)}_2))$ and the uncorrelated product $\rho(\boldsymbol{R}^{(1)}_1,\boldsymbol{R}^{(1)}_2)\,\rho(\boldsymbol{R}^{(2)}_2,\boldsymbol{R}^{(2)}_2)$. From $\rho((\boldsymbol{R}^{(1)}_1,\boldsymbol{R}^{(1)}_2),(\boldsymbol{R}^{(2)}_1,\boldsymbol{R}^{(2)}_2)) = A^2(\boldsymbol{R}^{(1)}_1,\boldsymbol{R}^{(1)}_2,\boldsymbol{R}^{(2)}_1,\boldsymbol{R}^{(2)}_2)$ [Eq. (20)], it can be shown that this differs from the uncorrelated product $(\phi^{(1)}_1(\boldsymbol{R}^{(1)}_1))^2(\phi^{(1)}_2(\boldsymbol{R}^{(1)}_2))^2(\phi^{(2)}_1(\boldsymbol{R}^{(2)}_1))^2(\phi^{(2)}_2(\boldsymbol{R}^{(2)}_2))^2$ obtained using the FE amplitude $\phi^{(1)}_1(\boldsymbol{R}^{(1)}_1)\phi^{(1)}_2(\boldsymbol{R}^{(1)}_2)$ for the FE (1) and $\phi^{(2)}_1(\boldsymbol{R}^{(2)}_1)\phi^{(2)}_2(\boldsymbol{R}^{(2)}_2)$ for the FE (2). The difference is the quantum correlation between the FEs.

[33] W. Press *et al.*, in *Numerical Recipes* (Cambridge University Press, Cambridge, 2007), pp. 143–144.

[34] B. L. Jones, R. H. Enns, and R. S. S., Bull. Math. Biol. **38**, 15 (1976).

[35] Computer code CPMD, IBM Corp., Armonk, NY 1990–2008; Max-Planck-Institut für Festkörperforschung, Stuttgart, Germany 1997–2001 (2011) [http://www.cpmd.org].

[36] J. P. Perdew, K. Burke, and M. Ernzerhof, Phys. Rev. Lett. **77**, 3865 (1996).

[37] S. K. Ghosh and B. M. Deb, Int. J. Quantum Chem. **22**, 871 (1982).

[38] B. Poirier, J. Chem. Phys **121**, 4501 (2004).

[39] The fact that we use the same variables (R_1 and P_1) for both atoms does not constitute a problem since the two distributions are well separated in space (Fig. 2).

[40] R. E. Wyatt, *Quantum Dynamics with Trajectories: Introduction to Quantum Hydrodynamics* (Interdisciplinary Applied Mathematics, Springer, New York, 2005).